Am J Transl Res 2018;10(8):2469-2479
www.ajtr.org /ISSN:1943-8141/AJTR0070923

Original Article

Collagen type V a2 (COL5A2) is decreased in steroid-induced necrosis of the femoral head

Fan Yang*, Pengbo Luo*, Hao Ding, Changqing Zhang, Zhenhong Zhu

*Department of Orthopedic Surgery, Shanghai Jiao Tong University Affiliated Sixth People's Hospital, Shanghai, China. *Equal contributors.*

Received December 13, 2017; Accepted July 6, 2018; Epub August 15, 2018; Published August 30, 2018

Abstract: Collagen is essential for bone adhesion and formation. In the present study, proteomic analysis suggested that collagen type V a2 (COL5A2) was significantly decreased in the necrotic area of patients with steroid-induced necrosis of the femoral head (ONFH). *In vitro*, the effects of methylprednisolone (MP) on the proliferation and differentiation of human bone marrow-derived mesenchymal stem cells (hBMSCs) were investigated. The expression of the osteogenic-related proteins, Runx2, alkaline phosphatase (ALP), osteocalcin (OC) and COL5A2 was significantly downregulated post-MP treatment. *In vivo* analyses revealed that post-MP treatment, rats showed typical signs of ONFH by micro-CT scanning and hematoxylin and eosin (H&E) staining. Immunohistochemical staining demonstrated that the expression of COL5A2 and vascular endothelial growth factor (VEGF) was significantly decreased post-MP treatment. In conclusion, the expression COL5A2 was lower in patients with steroid-induced ONFH, hence COL5A2 may be a promising therapeutic target for steroid induced ONFH treatment.

Keywords: Collagen type V a2, osteonecrosis of the femoral head, steroid

Introduction

In patients with osteonecrosis of the femoral head (ONFH) or avascular necrosis (AVN), the vascular supply in trabecular bone of the femoral head was limited, which could lead to osteocyte death, and ultimately articular surface collapse [1]. In the United States, the annual prevalence of ONFH in the year of 1995 is about 10,000 to 20,000 cases, whereas, the number has certainly augmented [1, 2]. As known, ONFH mainly affects patients aged between 30 to 50 years and severely affects their quality of lives [3] and steroid and alcohol abuse are well-known causes for non-traumatic ONFH [4, 5]. Previous studies suggested that osteonecrosis and bone regeneration disruption caused by mesenchymal stem cells (MSCs) imbalanced differentiation contributed to the pathogenesis of non-traumatic ONFH [3, 6, 7]. Nevertheless, the underlying mechanism is not fully understood.

Bone is a dense, specialized form of connective tissue, which, along with cartilage, makes up the skeletal system [8]. Collagen plays essential roles in bone adhesion and bone formation. A recent study suggested that targeting collagen type IV alpha 1 (COL4A1) promoted osteoblastic cells survival and extracellular matrix (ECM) formation [9]. Platelet rich plasma (PRP) and collagen sheet combination improved the reparable capacity post drilling of necrotic segment in patients with ONFH [10]. It suggested that COL2A1 mutation is involved in idiopathic ONFH, and its mutation is controversial in ONFH [11, 12]. Nano-hydroxyapatite collagen (nHAC) bone increased osteogenesis in rabbits [13]. These studies suggest that collagens are of vital importance in ONFH. However, their expression profile in ONFH remains unexplored.

Hanash *et al* proposed that proteomics analysis has the potential to identify proteins that played essential roles in clinical diagnosis and monitoring [14]. By using proteomic analysis, Tan *et al* identified four proteins which were specific highly expressed in patients with ONFH than those with rheumatoid arthritis, osteoarthritis, or fractures [15]. Moreover, by using this technique, Zhang *at al* demonstrated that chondroi-

Table 1. Characteristics of patients

Variables	Corticosteroids group
Patients/hips (n)	4/4
Age (years)	49.75±10.01
Male/female (patients)	2/2
Right/left (hips)	3/1
Ficat-Arlet stage	Stage III

Table 2. The design of dimethyl labeling

127C	128N	128C	129N	129C	130N	130C	131
1A	1B	2A	2B	3A	3B	4A	4B

A: The normal area bone tissue, B: The necrotic area bone tissue. 1-4: Patient number.

tin sulfate proteoglycans, cation transportation, and mobilization synthesis are involved in the pathogenesis of ONFH [16]. Therefore, the present study identified the expression profiles of collagens in patients with glucocorticoid-induced ONFH by using this technique.

Methods

Participants

A total of four steroid-induced ONFH patients (two females and two males, age: 49.75±10.01 years) who underwent total hip replacement surgery were included from April 2014 to February 2015 in the Department of Orthopedics, Sixth People's Hospital Affiliated to Shanghai Jiao Tong University, China (**Table 1**). All patients did not receive chemotherapy or radiotherapy before surgery. Informed written consent was obtained from each subject. The study protocol was approved by the Institutional Review Board of Shanghai Sixth People's Hospital affiliated Shanghai Jiao Tong University school of medicine. The present study was in accordance with the Helsinki Declaration [17].

Proteomic analysis

The procedure of proteomic evaluation was conducted according to previous study [18]. In brief, a volume of 1 cm^3 of the anterior femoral heads in the necrotic area and adjacent normal area were grinded, lysed and the supernatant was precipitated by acetone for digestion. The precipitated protein was digested to peptides by trypsin and dried by lyophilization. Afterwards, the peptides were labeled with Tandem mass tag (TMT), then the TMT labeled peptides was dried by evaporation and desalted onto an Empore C18 47-mm Disk (3 M, USA). Peptides were separated using 3 μM C18 ReproSil particles (Dr. Maisch, GmbH, Germany) and introduced into mass spectrometry (Agilent, USA). A linear gradient from 4% to 30% buffer B (buffer A, 0.1% formic acid in ddH_2O; buffer B, 0.1% formic acid in acetonitrile) was used for peptide separation. The resolution for MS (mass spectra) was 60,000. Raw data were processed using the MaxQuant software (USA) and peak lists were searched against the UniProt database (http://www.uniprot.org/). The labeling sequences are listed in **Table 2**.

Human bone marrow-derived mesenchymal stem cells (hBMSCs) culture

Bone marrow samples were obtained from patients who undergone hip arthroplasty, and hBMSCs were isolated as previous described [20, 21]. hBMSCs were cultured at a density of 5.0×10^5 cells/flask in α-modified minimum essential medium (α-MEM; Sigma-Aldrich, St. Louis, MO, USA) containing 10% fetal bovine serum (FBS; Gibco, Carlsbad, CA, USA) and 1% penicillin-streptomycin (Gibco, USA) at 37°C in a humidified atmosphere containing 5% CO_2. Forty-eight hours later, the medium was changed to remove non-adherent cells. hBMSCs were passaged at ~80% confluence and cells at the three to six passages were used for further experiments. The study protocol was approved by the Institutional Review Board of Shanghai Sixth People's Hospital. Informed written consent was obtained from each patient, and the experimental procedures were approved by the Institutional Review Board of Shanghai Jiao Tong University Affiliated Sixth People's Hospital (Shanghai, China).

Flow cytometry

The characteristic of hBMSCs was assessed by flow cytometry. In brief, a number of 5×10^5 hBMSCs were incubated and stained with mouse anti-human CD44-fluorescein isothiocyanate (FITC), CD29-FITC, CD34-FITC, CD90-FITC, and HLA-DR-FITC antibodies (all from eBioscience, USA, 1:200) in dark at room temperature for 20 min. Then, flow cytometry was performed using the FACSCalibur flow cytometer (Becton Dickinson, USA). FlowJo 7.6.5 software (Tree

Table 3. The primers used for RT-PCR

Genes	Forward primer sequence (5'-3')	Reverse primer sequence (5'-3')
COL5A2	CCGGGTCTAGCTGGTGAAAG	TCTCCTCTAGGTCCTAACGGG
Runx2	CCGAGACCAACCGAGTCATTTA	AAGAGGCTGTTTGACGCCAT
OC	TCAACAATGGACTTGGAGCCC	AGCTCGTCACAATTGGGGTT
ALP	CAAGGATGCTGGGAAGTCCG	CTCTGGGCGCATCTCATTGT
β-actin	GTCATCCATGGCGAACTGGT	CGTCATCCATGGCGAACTGG

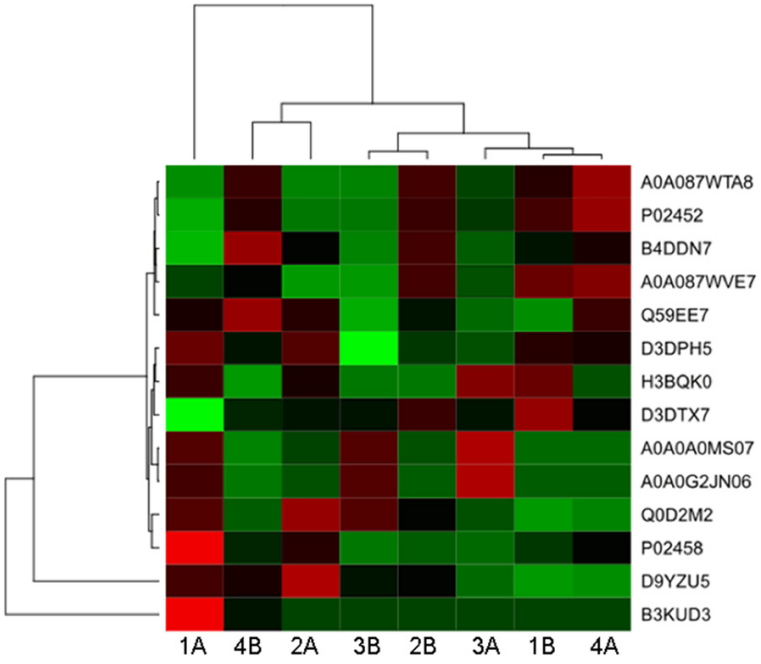

Figure 1. The heatmap of proteomic analysis. A stands for the adjacent normal tissue; B stands for the necrotic bone tissues. 1-4 means the patient number.

Star Inc., Ashland, OR, USA) was used for analysis.

Cell proliferation analysis

Approximately 5×10^3/well hBMSCs were plated in 96-well plates, and cells were divided to control and methylprednisolone (MP) groups. After treatment with 10^{-6} M MP, 10^{-5} M MP and 10^{-4} M MP for 72 h, cell proliferation was conducted by cell counting kit-8 (CCK-8; Beyotime, Nantong, China) according to manufacturer's instructions. The absorbance value was measured using a microplate reader (Bio-Rad, Hercules, CA, USA) at 450 nm.

Osteogenic differentiation in vitro

A number of 2×10^5/well hBMSCs were seeded in 24-well plates. When reaching at 70-80% confluence, culture medium was replaced with osteogenic differentiation medium which contains 10^{-2} M β-sodium glycerophosphate, 50 μg/ml L-ascorbic acid and 10^{-7} M dexamethasone.

Alkaline phosphatase (ALP) staining

ALP staining was performed on days 3 and 6 after the initiation of the differentiation cultures using the ALP staining kit (Blood Institute, Chinese Academy of Medical Sciences) according to manufacturer's instructions.

Alizarin red staining

Alizarin Red staining was performed to detect matrix mineralization deposition. Alizarin Red staining was performed on days 7 and 14 post osteogenic differentiation. In brief, hBMSCs were fixed by 95% ethanol for 10 min, and stained using Alizarin Red solution (1 g Tris and 0.1 g Alizarin Red, Sigma-Aldrich) in 100 ml ultrapure water (pH to 8.3 with HCl) at 37°C for 30 min. Then, the hBMSCs were visualized under a light microscope (Olympus, Japan) with five random sections.

Real-time quantitative polymerase chain reaction (RT-PCR)

After treatment, total RNA was extracted from using TRIzol reagent (Invitrogen, USA). Reverse transcription was performed to obtain cDNA using the High-Capacity Reverse Transcription kit (Invitrogen, USA). Then the expression of COL5A2, Runx2, Osteocalcin (OC) and ALP at the mRNA level was measured by RT-PCR. The procedures for RT-PCR were: 95°C for 30 s; 34 cycles at 95°C for 10 s and at 58°C for 30 s; and 72°C for 10 min. The expression of mRNAs was calculated by the $2^{-\Delta\Delta Ct}$ method, and β-actin was used as the reference gene. The primers are listed in **Table 3**. The experiments were performed in triplicate.

Table 4. The results of proteomic analysis

Protein IDs	Protein names	*P*-value
Q0D2M2	HIST1H2BC protein	0.641317
A0A0A0MS07	Ig gamma-1 chain C region (Fragment)	0.129329
A0A0G2JN06	Ig gamma-2 chain C region (Fragment)	0.108559
P02452	Collagen alpha-1 (I) chain	0.536247
P02458	Collagen alpha-1 (II) chain	0.162995
D3DPH5	Collagen, type V, alpha 2, isoform CRA b	0.036977*
A0A087WTA8	Collagen alpha-2 (I) chain	0.527214
Q59EE7	Pro-alpha-1 type V collagen variant (Fragment)	0.433474
B4DDN7	cDNA FLJ59839, highly similar to Homo sapiens biglycan (BGN), mRNA	0.182833
B3KUD3	cDNA FLJ39583 fis, clone SKMUS2004897, highly similar to ACTIN, ALPHA SKELETAL MUSCLE	0.485418
D9YZU5	Beta-globin	0.749597
A0A087WVE7	Scavenger receptor class F member 2	0.605093
D3DTX7	Collagen, type I, alpha 1, isoform CRA a	0.324097
H3BQK0	ATP-dependent RNA helicase DDX19B	0.180898

Compared between the necrosis bone and normal bone, *P<0.05.

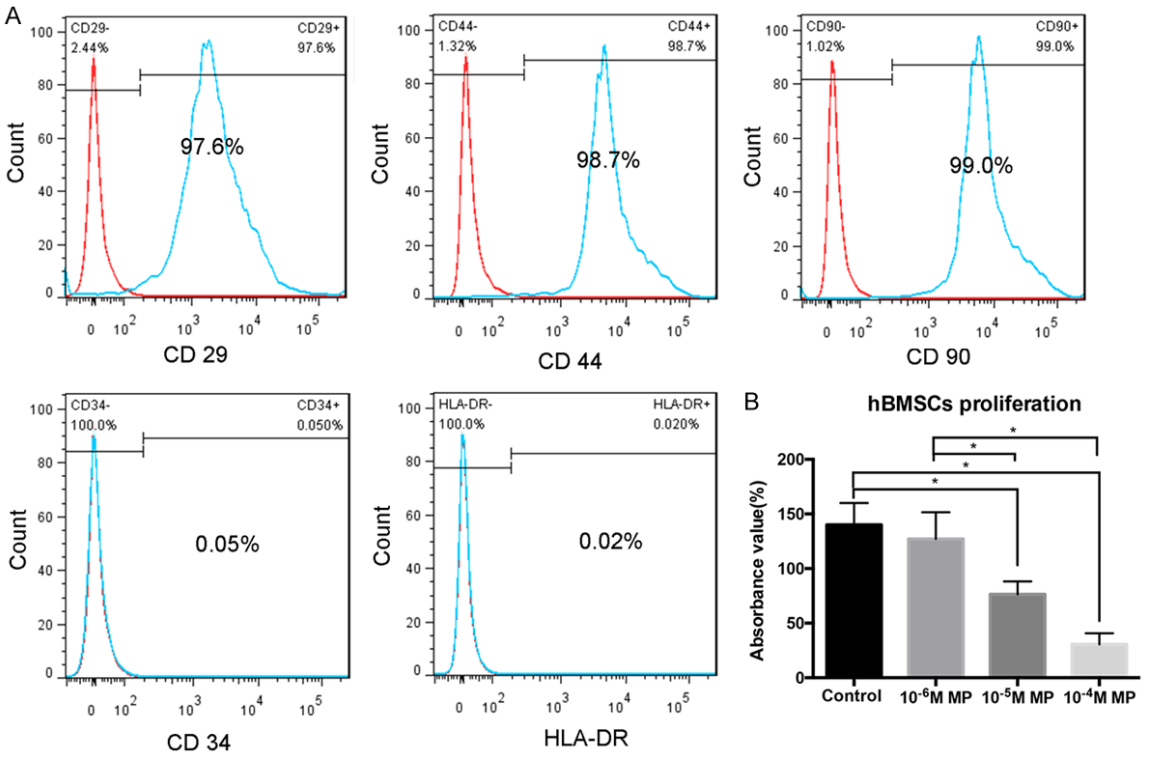

Figure 2. MP inhibited the proliferation of hBMSCs. A. The expression of surface markers (CD29, CD34, CD44, CD90 and HLA-DR) of hBMSCs and measured by flow cytometry. B. The cell viability of hBMSCs was detected by CCK-8. MP, methylprednisolone; hBMSC, human bone marrow-derived mesenchymal stem cells. The experiments were performed in triplicate. *P<0.05.

Animals

Thirty twelve-week-old male specific-pathogen-free Sprague-Dawley rats, weighing 300-450 g, were obtained from Silaike (Shanghai, China). The rats were randomized into control and MP groups. The rats in the MP group were intramuscular injected with methylprednisolone (30 mg/kg/day) for three weeks. Whereas, the rats in the control group were injected with normal

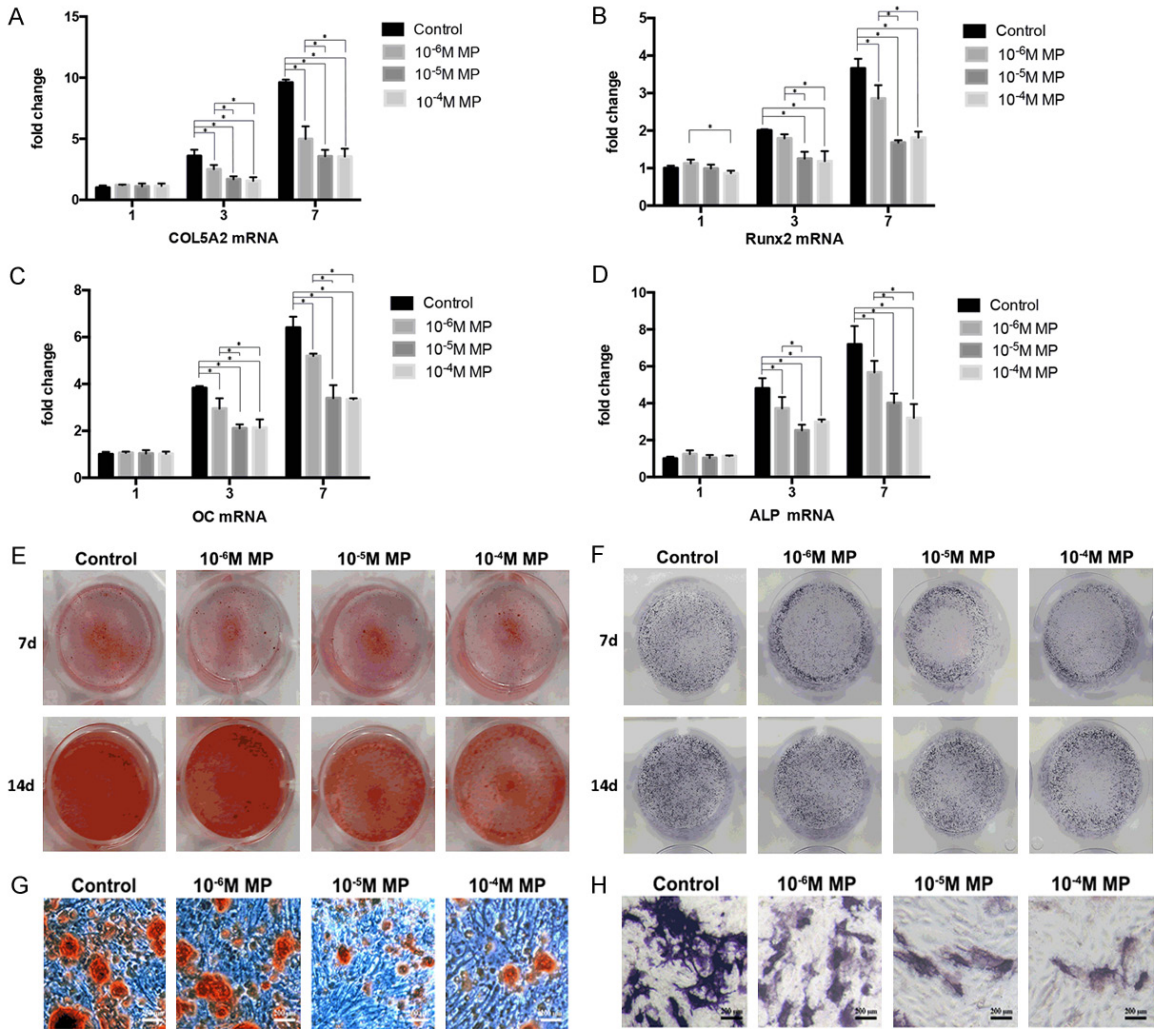

Figure 3. The expression of osteogenic related genes was decreased post-MP treatment. The expression of COL5A2 (A), Runx2 (B), OC (C), and ALP (D) at the mRNA level was measured by RT-PCR after 1, 3, and 7 days of incubation in the osteogenic medium of MP treated hBMSCs. Representative images of Alizarin red staining (E, G) and ALP staining (F, H) of MP treated hBMSCs. The experiments were performed in triplicate. *P< 0.05.

saline. The experiment procedure was approved by the Research Ethics Committee of the Shanghai Sixth People's Hospital-affiliated Shanghai Jiao Tong University, and performed in accordance with the Care and Use of Laboratory Animals protocols.

Histological analysis

After the rats were sacrificed, the femoral heads were harvested, decalcificated, embedded in paraffin and sectioned at a thickness of 5 μm in the coronal plane. Trabecular structure was evaluated by hematoxylin and eosin (HE) staining. The expression levels of OCN, Runx2, and CD31 were detected by immunohistochemistry. In brief, paraffin sections were dewaxed and boiled in 10 mM citrate buffer (pH 6.0) for 10 min. Endogenous peroxidase activity was blocked by hydrogen peroxide, and the non-specific-binding sites were blocked with normal goat serum for 1 h. Then, antibodies against COL5A2 (Gene Tex, United States, 1:100) and VEGF (Boshide, Wuhan, China, 1:100) were incubated overnight at 4°C. The bound antibodies were detected by the biotin-linked secondary antibodies and DAB chromogen-conjuncted streptavidin-conjugated HRP enzymes (Beyotime, China). Finally, the color was developed by 3-3'-diaminobenzidine, counterstained with hematoxylin, and the slides were observed under a laser confocal scanning microscope (Olympus). The integrated option density (IOD) of the target protein and the total

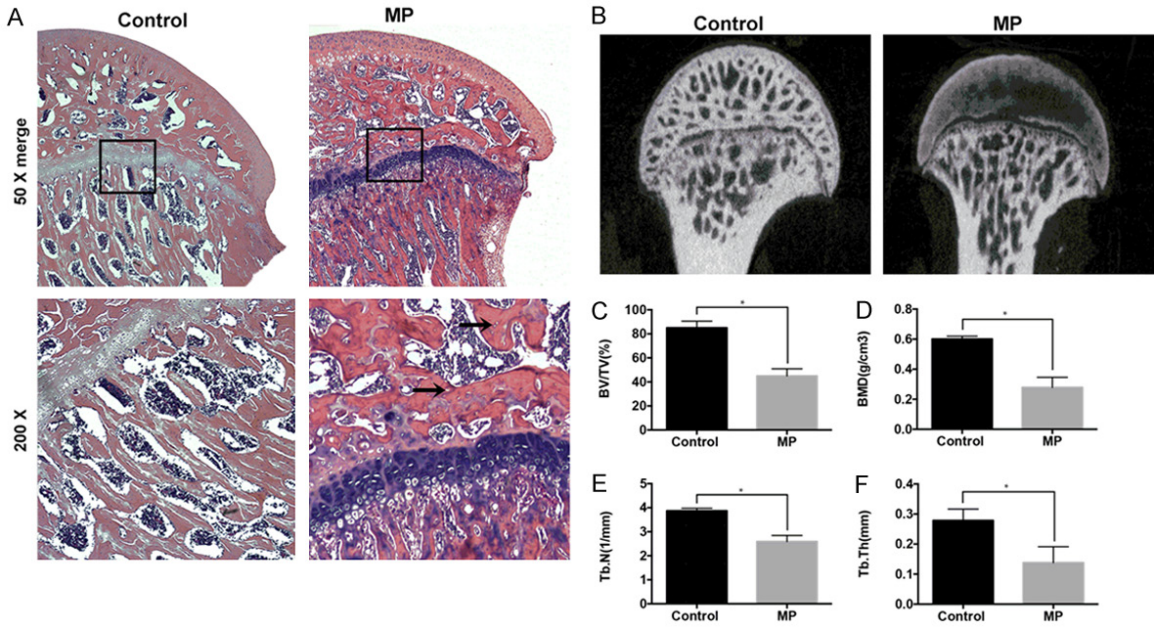

Figure 4. The morphogenic changes showed typical ONFH signs post-MP treatment. (A) HE staining of the coronal sections of representative femoral heads. The arrow indicates the empty bone lacuna. (B) Two-dimensional images of the coronal section of the femoral heads post-micro-CT scanning. Morphometric analysis showing callus parameters of the upper outer subchondral bone of the femoral heads, BV/TV (C), BMD (D), Tb.N (E) and Tb.Th (F). *P<0.05.

area of trabecular bones were measured using the software Image-Pro Plus (MEDIA CYBERNETICS, USA), and the mean density (IOD/area) was calculated.

Micro-CT scanning

The morphologic changes of femoral heads were measured by micro-CT scanning as previously described [20]. Briefly, the femoral head was scanned using a micro-CT scanner (Brooke, Germany) at a volex of 9 μm, and 2-D images were analyzed by CTAn software. The bone mineral density (BMD), bone volume per tissue volume (BV/TV), trabecular thickness (Tb.Th), and trabecular number (Tb.N) pertaining to trabecular bone parameters were quantified.

Angiography

After treatment, cardia was perfused with heparinized saline, and Microfil (Flow Tech, Inc., Inc., Carver, MA, USA) was injected through the abdominal aorta, after which, the rats were placed on the bed to ensure contrast agent polymerization at 4°C for 1 h. Femoral heads were fixed and decalcified. Afterwards, the samples were measured by micro-CT, and the femoral head vessels were reconstructed using CTVol software.

Statistical analysis

All the data are expressed as the mean ± standard deviation (SD). The Mann-Whitney U-test was used for comparisons between the two groups. One-way analysis of variance (ANOVA) or the Kruskal-Wallis test was applied for multiple comparisons between independent groups. Pairwise multiple comparisons were performed using the Tukey-Kramer or Scheffé *post hoc* test. Data analyses were performed using PASW Statistics 21 (SPSS, Chicago, IL, USA). A two-tail *p* value less than 0.05 was considered statistical significant.

Results

The expression of COL5A2 is decreased in the necrotic area of patients with steroid-induced ONFH

Protein was extracted from the necrotic area and their adjacent normal bone tissue in patients with steroid-induced ONFH. Proteomic chip was used to detect potential differentially expressed collagens. As depicted in **Figure 1** and **Table 4**, the content of COL5A2 in the necrotic area was significantly lowered than that in the normal tissues (P<0.05). These results suggest that COL5A2 was downregulat-

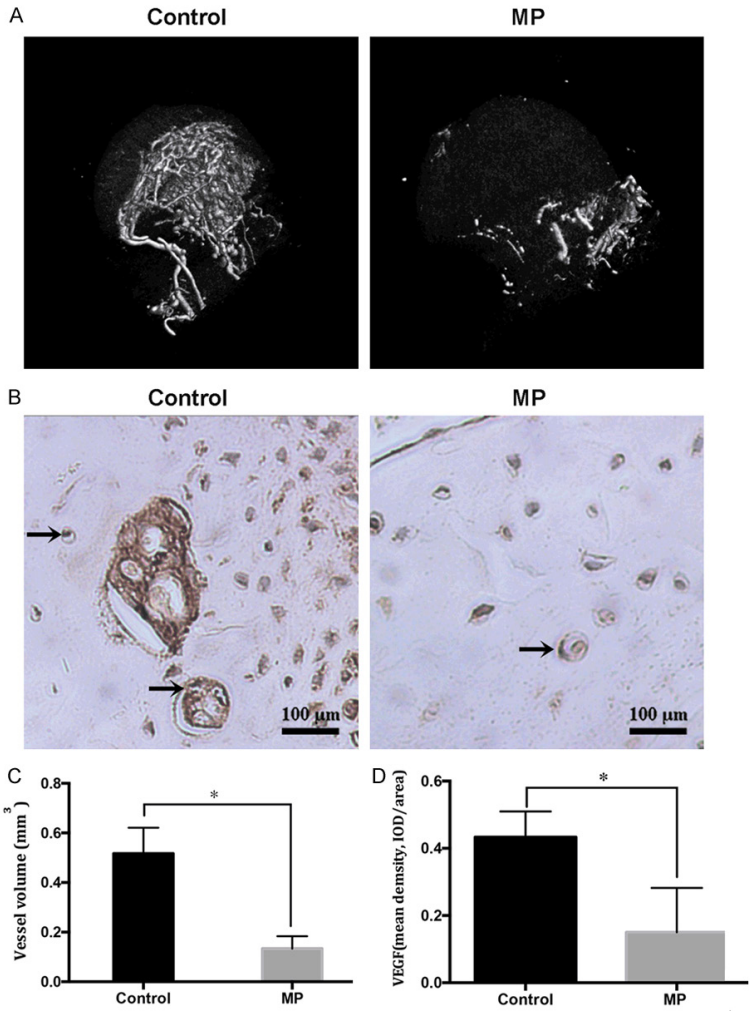

Figure 5. The number of blood vessels was decreased post-MP treatment. (A) Representative images of 3D microangiography of femoral heads were evaluated by micro-CT scanning. (B) Representative images of immunohistochemical staining of VEGF in the femoral heads, arrows indicate VEGF expression. Quantification of total volume of blood vessels (C) in the femoral heads and mean density of VEGF (D) in the femoral head slices of each group. *P<0.05.

ed in the development of *steroid-induced* ONFH.

MP inhibits hBMSCs proliferation, osteogenic differentiation and decreases COL5A2 expression in vitro

As shown in **Figure 2A**, the isolated cells showed typical characteristics of hBMSCs which showed high expression of CD44, CD90, and CD29 and low expression of CD39 and HLA-DR. The impact of MP in hBMSCs proliferation was assessed. Post incubation with MP for 72 h, the proliferation assay revealed that MP inhibited hBMSCs proliferation in a dose dependent manner (**Figure 2B**). Moreover, the expression of osteogenic related gens was measured by real-time PCR. As expected, the expression of Runx2, OC, ALP, and COL5A2 was significantly downregulated post-MP incubation after osteogenic differentiation at day 3 and 7 (all P<0.05, **Figure 3A-D**). Alizarin red staining showed that MP decreased the number of calcium nodules compared with control group post-osteogenic differentiation at the day 7 and 14 (**Figure 3E**, **3G**). Similar results were obtained from ALP staining, in which the dark-blue NBT-formazan decreased with increasing MP concentration post osteogenic differentiation at day 3 and 6 (**Figure 3F**, **3H**).

The expression of COL5A2 was decreased during the process of MP induced ONFH in rats

Six weeks following the first injection of MP, hematoxylin and eosin (HE) staining was used to determine the trabecular changes in the subchondral area of the femoral heads, which showed typical signs of ONFH (**Figure 4A**). In consistent to the HE staining, micro-CT scan showed a large amount of bone loss compared to the control group (**Figure 4B**). Moreover, there was a significant reduction of bone volume per tissue volume (BV/TV), trabecular thickness (Tb.Th), and trabecular number (Tb.N) in MP group compare with control group (all P<0.05, **Figure 4C**, **4E**, **4F**). A significant decrease of bone mass was observed in the bone mineral density (BMD) in the MP group compared with the control group (P< 0.05; **Figure 4D**). The reconstructed 3D micro-CT images revealed that the blood vessels in the femoral head in the MP group was significantly decreased compared with control group (P<0.05, **Figure 5A**, **5C**). Furthermore, the expression of VEGF, a typical indicator for vascularization, was detected by immunohisto-

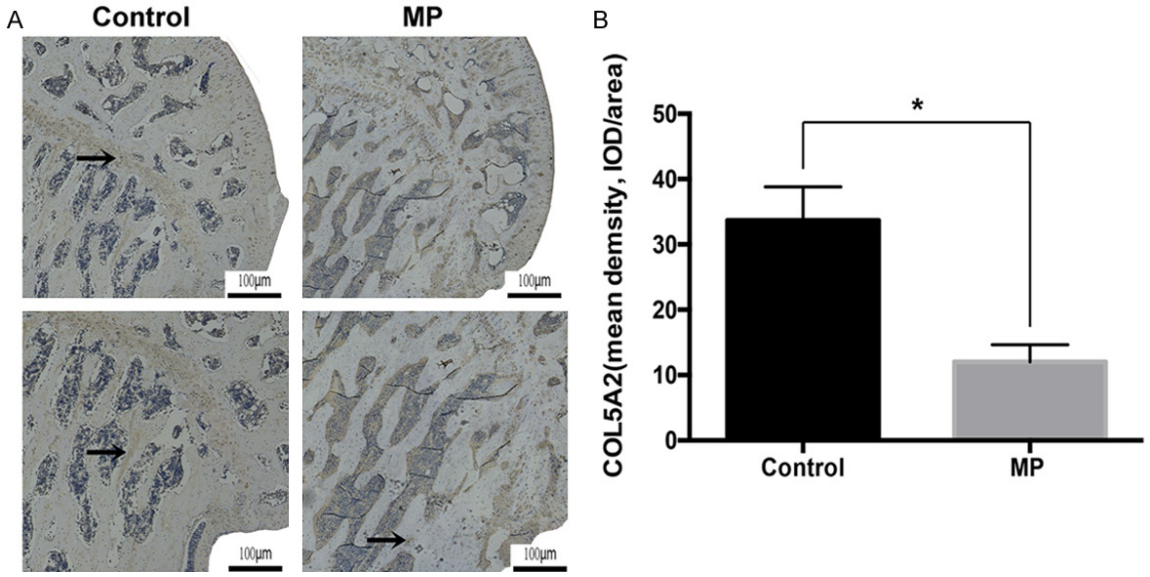

Figure 6. The expression of COL5A2 was decreased post-MP. A. Representative images of immunohistochemical staining of COL5A2 in the coronal sections of femoral heads. B. Quantification of mean density of COL5A2. *P<0.05.

chemistry staining. In agreement with micro-CT scanning, the expression of VEGF was significantly lowered in the MP group in contrast with the control group (**Figure 5B**, **5D**). Next, we detected the expression of COL5A2 by immunohistochemistry. The results showed that few positive staining signals were found in the osteonecrotic area and less positive staining signals were detected in the surviving trabeculae in the MP group compared to the control group (P<0.05, **Figure 6A**, **6B**).

Discussion

The profile of collagens in ONFH has not been elucidated, in the present study, proteomic analysis revealed that the expression COL5A2 was significantly decreased, indicating COL5A2 may be therapeutic target for the treatment of ONFH.

The balanced production and degradation of matrix proteins in extracellular matrix (ECM) is essential for the homeostasis of tissues [22, 23]. Osteoblast interaction with the bone ECM plays an important role for osteoblasts anchorage, proliferation, differentiation, and function [24, 25]. Bone cell cultures have the capacity to produce a wide range of matrix proteins, including collagen types I, III, IV, V, and fibronectin [26]. COL5 is synthesized and deposited in the ECM, where it crosslinked with COL1, 3 and COL6, to form the collagenous tissue scaffold [27]. Dun's *et al* revealed that COL5A2 in the ECM played critical roles in regulating cell spreading and actin skeleton formation in the early stage of osteoblast differentiation [28]. Abnormal remodeling of the extracellular matrix may produce pathological changes. In the present study, proteomic analysis demonstrated that COL5A2 was significantly lowered in ONFH patients, and its downregulation was confirmed both *in vitro* and *in vivo*. These findings indicated that imbalanced COL5A2 expression may contribute to the pathogenesis of ONFH.

Glucocorticoids have detrimental effects on osteoblasts, osteoclasts, and osteocytes [31]. These side effects are believed partly due to suppression of osteogenic differentiation of mesenchymal stem cells and apoptosis of osteoblasts and osteocytes [32]. At early stages, ONFH is mainly characterized by the death of osteocytes, then the reparative reaction of necrotic bone is initiated. The imbalance between osteoclast-mediated bone resorption and osteoblast-mediated bone reformation leads to structural damage and collapse of the femoral head [33]. As osteonecrosis is the representative pathological change in ONFH, most studies of ONFH have focused on the mechanism of damage to the bone and the bone marrow in the femoral head [34-36]. In the present study, the expression of osteogenic-associated genes, such as Runx2, and ALP were inhibited,

which is consistent with previous studies [37, 38].

Glucocorticoids decrease the vessel volume and blood supply of femoral heads. Recent study revealed that glucocorticoids can directly injure endothelial cells and decrease the expression of VEGF, which is an essential angiogenic factor for angiogenesis in endothelial cells [39, 40]. Collagens serve as key components for maintaining the structural integrity and for mediating thrombosis through interaction with platelets in the blood vessel walls [41, 42]. Fukuda *et al* found that COL5 inhibited the proliferation of human umbilical vein endothelial cells, but it did not affect the proliferation of vascular smooth muscle cells [43]. COL5 selectively inhibited human endothelial cell proliferation and may promote cell detachment by the disassembly of F-actin filaments, and cells started to proliferate when re-cultured on COL1 [27]. However, a recent study revealed that COL5A2 plays essential roles in maintaining the aortic arch integrity [29]. Moreover, heterozygous mutation in COL5a2 gene could lead to connective tissue hyperelasticity and joint instability [30]. This study showed that MP inhibited the expression of COL5A2, reduced the amount of bone tissue and lowered the expression of VEGF, one potential translational value of this finding is that COL5A2 deficiency may participate in the avascular and joint deterioration progress of ONFH. Whereas, the underlying mechanism of how COL5A2 participates in the pathogenesis of ONFH, and whether enhancement of the expression of COL5A2 could promote the healing process of necrotic tissue in ONFH are still unknown. Further studies using transgenic COL5A2 BMSCs are needed to unveil the potential role of COL5A2 in ONFH.

In conclusion, by applying proteomic analysis, this study demonstrated that the COL5A2 content in the steroid-induced osteonecrosis region was significantly decreased compared to their adjacent normal areas. These findings suggested that steroid-induced reduction in COL5A2 may attribute to the progression of osteonecrosis, nevertheless more work is needed to unveil the role of COL5A2 in the pathogenesis of ONFH.

Acknowledgements

This study was funded by the National Natural Science Foundation of China (No 81272004).

Disclosure of conflict of interest

None.

Address correspondence to: Changqing Zhang and Zhenhong Zhu, Department of Orthopedic Surgery, Shanghai Jiao Tong University Affiliated Sixth People's Hospital, Shanghai, China. Tel: +00861-3003104089; E-mail: zhangcq@sjtu.edu.cn (CQZ); Tel: +008618930174588; E-mail: zzhwz@21cn.com (ZHZ)

References

[1] Gou WL, Lu Q, Wang X, Wang Y, Peng J and Lu SB. Key pathway to prevent the collapse of femoral head in osteonecrosis. Eur Rev Med Pharmacol Sci 2015; 19: 2766-2774.

[2] Mont MA and Hungerford DS. Non-traumatic avascular necrosis of the femoral head. J Bone Joint Surg Am 1995; 77: 459-474.

[3] Wei B, Wei W, Zhao B, Guo X and Liu S. Long non-coding RNA HOTAIR inhibits miR-17-5p to regulate osteogenic differentiation and proliferation in non-traumatic osteonecrosis of femoral head. PLoS One 2017; 12: e0169097.

[4] Kubo T, Ueshima K, Saito M, Ishida M, Arai Y and Fujiwara H. Clinical and basic research on steroid-induced osteonecrosis of the femoral head in Japan. J Orthop Sci 2016; 21: 407-413.

[5] Gan D and Zhang C. Research progress of alcohol-induced osteonecrosis of femoral head. Zhongguo Xiu Fu Chong Jian Wai Ke Za Zhi 2013; 27: 365-368.

[6] Ng VY, Granger JF and Ellis TJ. Calcium phosphate cement to prevent collapse in avascular necrosis of the femoral head. Med Hypotheses 2010; 74: 725-726.

[7] Lee JS, Lee JS, Roh HL, Kim CH, Jung JS and Suh KT. Alterations in the differentiation ability of mesenchymal stem cells in patients with nontraumatic osteonecrosis of the femoral head: comparative analysis according to the risk factor. J Orthop Res 2006; 24: 604-609.

[8] Kimmel DB and Jee WS. Bone cell kinetics during longitudinal bone growth in the rat. Calcif Tissue Int 1980; 32: 123-133.

[9] Li QS, Meng FY, Zhao YH, Jin CL, Tian J and Yi XJ. Inhibition of microRNA-214-5p promotes cell survival and extracellular matrix formation by targeting collagen type IV alpha 1 in osteoblastic MC3T3-E1 cells. Bone Joint Res 2017; 6: 464-471.

[10] Samy AM. Management of osteonecrosis of the femoral head: a novel technique. Indian J Orthop 2016; 50: 359-365.

[11] Sakamoto Y, Yamamoto T, Miyake N, Matsumoto N, Iida A, Nakashima Y; Research Com-

mittee on Idiopathic Osteonecrosis of the Femoral Head of the Ministry of Health, Labour and Welfare of Japan, Iwamoto Y, Ikegawa S. Screening of the COL2A1 mutation in idiopathic osteonecrosis of the femoral head. J Orthop Res 2017; 35: 768-774.

[12] Kannu P, O'Rielly DD, Hyland JC and Kokko LA. Avascular necrosis of the femoral head due to a novel C propeptide mutation in COL2A1. Am J Med Genet A 2011; 155A: 1759-1762.

[13] Sun W, Li Z, Shi Z, Zhang N, Li Y and Cui F. Effect of nano-hydroxyapatite collagen bone and marrow mesenchymal stem cell on treatment of rabbit osteonecrosis of the femoral head defect. Zhongguo Xiu Fu Chong Jian Wai Ke Za Zhi 2005; 19: 703-706.

[14] Hanash S. Disease proteomics. Nature 2003; 422: 226-232.

[15] Xu DZ, Cai HD, Ma XY, Li YQ, Lu XZ, Yu HY, Sun AM, Zhao LF, Zhang LY and Gao XH. Comparative analysis of the efficacies of entecavir capsules and lamivudine in chronic hepatitis B patients. Zhonghua Gan Zang Bing Za Zhi 2013; 21: 886-890.

[16] Zhang H, Zhang L, Wang J, Ma Y, Zhang J, Mo F, Zhang W, Yan S, Yang G and Lin B. Proteomic analysis of bone tissues of patients with osteonecrosis of the femoral head. OMICS 2009; 13: 453-466.

[17] General Assembly of the World Medical Association. World medical association declaration of helsinki: ethical principles for medical research involving human subjects. J Am Coll Dent 2014; 81: 14-18.

[18] Zhuang G, Yu K, Jiang Z, Chung A, Yao J, Ha C, Toy K, Soriano R, Haley B, Blackwood E, Sampath D, Bais C, Lill JR and Ferrara N. Phosphoproteomic analysis implicates the mTORC2-FoxO1 axis in VEGF signaling and feedback activation of receptor tyrosine kinases. Sci Signal 2013; 6: ra25.

[19] Wisniewski JR, Zougman A, Nagaraj N and Mann M. Universal sample preparation method for proteome analysis. Nat Methods 2009; 6: 359-362.

[20] Zhang YL, Yin JH, Ding H, Zhang W, Zhang CQ and Gao YS. Vitamin K2 prevents glucocorticoid-induced osteonecrosis of the femoral head in rats. Int J Biol Sci 2016; 12: 347-358.

[21] Neve A, Corrado A and Cantatore FP. Osteocalcin: skeletal and extra-skeletal effects. J Cell Physiol 2013; 228: 1149-1153.

[22] Humphrey JD, Dufresne ER and Schwartz MA. Mechanotransduction and extracellular matrix homeostasis. Nat Rev Mol Cell Biol 2014; 15: 802-812.

[23] Tan RJ and Liu Y. Matrix metalloproteinases in kidney homeostasis and diseases. Am J Physiol Renal Physiol 2012; 302: F1351-1361.

[24] Alford AI, Kozloff KM and Hankenson KD. Extracellular matrix networks in bone remodeling. Int J Biochem Cell Biol 2015; 65: 20-31.

[25] He F, Liu X, Xiong K, Chen S, Zhou L, Cui W, Pan G, Luo ZP, Pei M and Gong Y. Extracellular matrix modulates the biological effects of melatonin in mesenchymal stem cells. J Endocrinol 2014; 223: 167-180.

[26] Grzesik WJ and Robey PG. Bone matrix RGD glycoproteins: immunolocalization and interaction with human primary osteoblastic bone cells in vitro. J Bone Miner Res 1994; 9: 487-496.

[27] Mak KM, Png CY and Lee DJ. Type V collagen in health, disease, and fibrosis. Anat Rec (Hoboken) 2016; 299: 613-629.

[28] Hong D, Chen HX, Yu HQ, Liang Y, Wang C, Lian QQ, Deng HT and Ge RS. Morphological and proteomic analysis of early stage of osteoblast differentiation in osteoblastic progenitor cells. Exp Cell Res 2010; 316: 2291-2300.

[29] Park AC, Phan N, Massoudi D, Liu Z, Kernien JF, Adams SM, Davidson JM, Birk DE, Liu B and Greenspan DS. Deficits in Col5a2 expression result in novel skin and adipose abnormalities and predisposition to aortic aneurysms and dissections. Am J Pathol 2017; 187: 2300-2311.

[30] Johnston JM, Connizzo BK, Shetye SS, Robinson KA, Huegel J, Rodriguez AB, Sun M, Adams SM, Birk DE and Soslowsky LJ. Collagen V haploinsufficiency in a murine model of classic Ehlers-Danlos syndrome is associated with deficient structural and mechanical healing in tendons. J Orthop Res 2017; 35: 2707-2715.

[31] Tan G, Kang PD and Pei FX. Glucocorticoids affect the metabolism of bone marrow stromal cells and lead to osteonecrosis of the femoral head: a review. Chin Med J (Engl) 2012; 125: 134-139.

[32] Hong L, Wei N, Joshi V, Yu Y, Kim N, Krishnamachari Y, Zhang Q and Salem AK. Effects of glucocorticoid receptor small interfering RNA delivered using poly lactic-co-glycolic acid microparticles on proliferation and differentiation capabilities of human mesenchymal stromal cells. Tissue Eng Part A 2012; 18: 775-784.

[33] Weinstein RS, Wan C, Liu Q, Wang Y, Almeida M, O'Brien CA, Thostenson J, Roberson PK, Boskey AL, Clemens TL and Manolagas SC. Endogenous glucocorticoids decrease skeletal angiogenesis, vascularity, hydration, and strength in aged mice. Aging Cell 2010; 9: 147-161.

[34] Wang C, Peng J and Lu S. Summary of the various treatments for osteonecrosis of the femoral head by mechanism: a review. Exp Ther Med 2014; 8: 700-706.

[35] Zhang Y, Yin J, Ding H, Zhang C and Gao YS. Vitamin K2 ameliorates damage of blood vessels by glucocorticoid: a potential mechanism for its protective effects in glucocorticoid-induced osteonecrosis of the femoral head in a rat model. Int J Biol Sci 2016; 12: 776-785.
[36] Guo KJ, Zhao FC, Guo Y, Li FL, Zhu L and Zheng W. The influence of age, gender and treatment with steroids on the incidence of osteonecrosis of the femoral head during the management of severe acute respiratory syndrome: a retrospective study. Bone Joint J 2014; 96-B: 259-262.
[37] Baniwal SK, Shah PK, Shi Y, Haduong JH, Declerck YA, Gabet Y and Frenkel B. Runx2 promotes both osteoblastogenesis and novel osteoclastogenic signals in ST2 mesenchymal progenitor cells. Osteoporos Int 2012; 23: 1399-1413.
[38] Hu N, Feng C, Jiang Y, Miao Q and Liu H. Regulative effect of mir-205 on osteogenic differentiation of bone mesenchymal stem cells (BMSCs): possible role of SATB2/Runx2 and ERK/MAPK pathway. Int J Mol Sci 2015; 16: 10491-10506.
[39] Yano A, Fujii Y, Iwai A, Kageyama Y and Kihara K. Glucocorticoids suppress tumor angiogenesis and in vivo growth of prostate cancer cells. Clin Cancer Res 2006; 12: 3003-3009.
[40] Mitre-Aguilar IB, Cabrera-Quintero AJ and Zentella-Dehesa A. Genomic and non-genomic effects of glucocorticoids: implications for breast cancer. Int J Clin Exp Pathol 2015; 8: 1-10.
[41] Poiani GJ, Tozzi CA, Thakker-Varia S, Choe JK and Riley DJ. Effect of glucocorticoids on collagen accumulation in pulmonary vascular remodeling in the rat. Am J Respir Crit Care Med 1994; 149: 994-999.
[42] Soe K and Delaisse JM. Glucocorticoids maintain human osteoclasts in the active mode of their resorption cycle. J Bone Miner Res 2010; 25: 2184-2192.
[43] Fukuda K, Koshihara Y, Oda H, Ohyama M and Ooyama T. Type V collagen selectively inhibits human endothelial cell proliferation. Biochem Biophys Res Commun 1988; 151: 1060-1068.